Author Manuscript

Author Manuscript

Author Manuscript

Author Manuscript

HHS Public Access

Author manuscript

Nat Commun. Author manuscript; available in PMC 2013 December 24.

Published in final edited form as:

Nat Commun. 2013 ; 4: 2037. doi:10.1038/ncomms3037.

Antagonism between binding site affinity and conformational dynamics tunes alternative *cis*-interactions within Shp2

Jie Sun[1,2,3], **Shaoying Lu**[2], **Mingxing Ouyang**[2], **Li-Jung Lin**[2], **Yue Zhuo**[2], **Bo Liu**[2], **Shu Chien**[5], **Benjamin G. Neel**[6], and **Yingxiao Wang**[1,2,3,4,7,*]

[1]Department of Molecular and Integrative Physiology, University of Illinois at Urbana-Champaign, Urbana, IL 61801, USA

[2]Department of Bioengineering, University of Illinois at Urbana-Champaign, Urbana, IL 61801, USA

[3]The Beckman Institute for Advanced Science and Technology, University of Illinois at Urbana-Champaign, Urbana, IL 61801, USA

[4]Neuroscience Program, Center for Biophysics and Computational Biology, and Institute for Genomic Biology, University of Illinois at Urbana-Champaign, Urbana, IL 61801, USA

[5]Departments of Bioengineering and Medicine, University of California, San Diego, La Jolla, CA 92093, USA

[6]Campbell Family Cancer Research Institute, Ontario Cancer Institute, Princess Margaret Hospital, University Health Network, and Department of Medical Biophysics, University of Toronto, Toronto, Ontario, Canada M5G 2M9

[7]Departments of Bioengineering, University of California, San Diego, La Jolla, CA 92093, USA

Abstract

Protein functions are largely affected by their conformations. This is exemplified in proteins containing modular domains. However, the evolutionary dynamics that define and adapt the conformation of such modular proteins remain elusive. Here we show that *cis*-interactions between the C-terminal phosphotyrosines and SH2 domain within the protein tyrosine phosphatase Shp2 can be tuned by an adaptor protein, Grb2. The competitiveness of two phosphotyrosines, namely pY542 and pY580, for *cis*-interaction with the same SH2 domain is governed by an antagonistic combination of contextual amino acid sequence and position of the phosphotyrosines. Specifically, pY580 with the combination of a favorable position and an adverse sequence has an overall advantage over pY542. Swapping the sequences of pY542 and pY580 results in one dominant form of *cis*-interaction and subsequently inhibits the *trans*-regulation by Grb2. Thus, the

Users may view, print, copy, and download text and data-mine the content in such documents, for the purposes of academic research, subject always to the full Conditions of use:http://www.nature.com/authors/editorial_policies/license.html#terms

*To whom correspondence should be addressed: Yingxiao Wang, Ph. D., yiw015@eng.ucsd.edu, Tel: 858-534-5256.

Author contributions: J.S., S.L., S.C. and Y.W. designed the experiments. J.S., M.O., L.L., Y.Z., and B.L. performed the experiments. J.S. and S.L. analyzed the data. J.S., B.G.N, S.C. and Y.W. wrote the manuscript.

Competing financial interests: The authors declare no competing financial interests.

Author Manuscript Author Manuscript Author Manuscript Author Manuscript

antagonistic combination of sequence and position may serve as a basic design principle for proteins with tunable conformations.

INTRODUCTION

Intramolecular interactions within proteins (*cis*-interactions) and allosteric regulations by neighboring molecules (*trans*-interactions) are common ways to regulate protein functions. One mode of *cis*-interaction is autoinhibition in which a *cis*-regulatory element interacts with and inhibits the catalytic/functional domain. Disruption of the *cis*-interaction usually involves a neighboring molecule *trans*-interacting with the *cis*-regulatory element and relieving the autoinhibition to activate the protein [1]. In these interactions, modularity is a recurring theme to regulate diverse functions of proteins [2]. While the specific sequence and position of DNA *cis*-regulatory elements have been intensively studied to elucidate their roles in regulating gene expression [3-5], the basic principles underlying how protein modules are designed and arranged to govern their conformations and functions remain largely elusive. X-ray crystallography, NMR spectroscopy, and single-molecule spectroscopic methods can provide details of molecular conformations *in vitro*, but have limited capability in live cells, particularly for proteins containing multiple interacting domains and capable of adopting diverse conformations [6]. Genetically-encoded reporters based on fluorescent proteins (FPs) and fluorescence resonance energy transfer (FRET) allow the monitoring of the molecular interactions and conformational changes in live cells with high spatiotemporal resolution[7-10]. In this study we employed FRET to study the *cis*- and *trans*-interactions of Src homology 2 domain-containing protein tyrosine phosphatase 2 (Shp2).

Encoded by *PTPN11*, Shp2 is a protein tyrosine phosphatase (PTP) that plays a critical role in various pathophysiological processes [11-13]. Mutations of *PTPN11* cause Noonan Syndrome [14], LEOPARD syndrome [15], and juvenile myelomonocytic leukemia [16,17]. Structurally, Shp2 consists of two SH2 domains (N-SH2 and C-SH2), a PTP domain, and a C-terminal tail (C-tail) containing two major tyrosine sites (Y542 and Y580) [18]. By incorporating nonhydrolysable phosphonomethylene phenylalanine (Pmp) at either Y542 or Y580, it has been suggested that these unnatural chemical modifications mimicking phosphotyrosines may cause the coupling between intramolecular domains *in vitro* to alter phosphatase activity of Shp2 [19]. However, it is unclear how the protein modules within Shp2 are designed for the *cis*-regulation and coordination of physiological Shp2 functions in live cells.

We have developed a FRET-based reporter to visualize conformational changes of Shp2 and their underlying regulation mechanisms in live cells. Our results indicate that an antagonistic combination of contextual amino acid (aa) sequence and position of two tyrosine sites (Y542 and Y580) within Shp2 facilitates the effective tuning of Shp2 *cis*-interactions by Grb2-mediated *trans*-regulation. The disruption of this antagonistic combination results in the inhibition of *trans*-regulation of Shp2 conformations and reprograms kinetics of the downstream ERK signaling. We suggest that this antagonistic combination of sequence and position may serve as a basic design principle for proteins with tunable conformations and functions.

Author Manuscript Author Manuscript Author Manuscript Author Manuscript

RESULTS

FRET-based reporter reveals *cis*-interaction of Shp2 *in vitro*

We studied the Shp2 conformations by engineering FRET reporters containing a full length wild-type (WT) Shp2 flanked by a sensitive FRET pair, an enhanced cyan FP (ECFP) and a yellow FP variant (YPet) [20] (Fig. 1a). The purified WT reporter *in vitro* can be phosphorylated by platelet-derived growth factor receptor (PDGFR) β kinase at both Y542 and Y580 (Fig. 1b), concomitant with an enhanced FRET level represented by an increase in YPet and a decrease in ECFP emission (Fig. 1c). The sustained FRET increase of the WT reporter suggests that PDGFRβ kinase activity is dominant over intrinsic phosphatase activity of the Shp2 reporter (Fig. 1d). Consistently, the incubation with extra amount of kinase didn't cause further increase of the overall level of FRET signals (Supplementary Fig. S1a). In contrast, PDGFRβ caused the phosphorylation but not FRET change of a mixture containing ECFP-Shp2 (ECFP fused to Shp2) and Shp2-YPet (YPet fused to Shp2) (Supplementary Fig. S1b), indicating minimal intermolecular interactions (*trans*-interactions) between different copies of Shp2 reporters. Furthermore, the PDGFRβ-induced FRET increase was lost in the YDF reporter with mutations of both Y542 and Y580 (Fig. 1d), which still has intact SH2 domains capable of *trans*-interaction with the phosphorylated Y1009 of PDGFRβ in the assay [21]. Therefore, the FRET response of WT reporter cannot be attributed to its interaction with PDGFRβ either, and must arise from intramolecular interactions (*cis*-interactions) within Shp2.

C-SH2 dominates the *cis*-interaction *in vitro*

The PDGFRβ-induced FRET response was eliminated by YDF or the double SH2 domain mutant (RDL) (Fig. 1d), suggesting that the *cis*-interactions within Shp2 are mediated by its SH2 domains and phosphotyrosines at C-tail. Single C-SH2 mutation (R138L), but not N-SH2 mutation (R32L), eliminated the PDGFRβ-induced FRET increase (Fig. 1e), indicating that C-SH2 is essential for the *cis*-interaction. Y580F, but not Y542F mutation, blocked most FRET increase (Fig. 1f), even though the phosphorylation of these two mutants was similar to that of WT reporters (Fig. 1g). Therefore, the FRET response of WT reporter *in vitro* is mainly due to the *cis*-interaction between C-SH2 and phosphorylated Y580 (pY580) (Fig. 1h). This notion is further supported by the obvious FRET response of a mutant disrupting the functions of both N-SH2 and Y542 (R32LY542F) (Supplementary Fig. S1c).

cis-Interaction competitiveness of the phosphotyrosines

Interestingly, there was a consistent although minor FRET response of the Y580F reporter (Fig. 1f and inset), suggesting that phosphorylated Y542 (pY542) may also undergo *cis*-interaction with C-SH2 in the absence of pY580 but only yield a weak FRET change. The reason for this weak FRET may come from the 51aa-long flexible C-tail region of the Y580F reporter between pY542 (the C-SH2 binding site) and YPet (the FRET acceptor) (Fig. 2a), in contrast to the short 13aa-region between pY580 and YPet in WT and Y542F reporters (Fig. 1h). Indeed, truncating this 51aa-long region (Δ580) to 13aa (Fig. 2a) caused a substantial FRET increase upon PDGFRβ incubation (Fig. 2b), which can be abolished by additional C-SH2 (R138L) but not N-SH2 (R32L) mutation (Supplementary Fig. S1d). These results confirmed that the *cis*-interaction between pY542 and C-SH2 can occur in the

Author Manuscript Author Manuscript Author Manuscript Author Manuscript

absence of pY580 (Fig. 2a). However, pY580 dominates the *cis*-interactions with C-SH2 in the population of WT reporters because the conversion of weak-FRET population, if any, to high FRET by Y542F mutation did not cause any significant increase in the overall FRET response (Fig. 1d, f and h). Since both tyrosine sites are phosphorylated in WT reporter (Fig. 1g), we suspect that the amino acid sequence surrounding pY580 has a higher affinity binding to C-SH2. Surprisingly, direct affinity measurement of the isolated pY542 or pY580 peptide toward C-SH2 by surface plasmon resonance (SPR) revealed a much higher binding affinity between pY542 and C-SH2 (Fig. 2c and Table 1). Furthermore, when the Y542 sequence was truncated so that it was replaced by the relocated Y580 sequence (Δ542, Fig. 2a), no FRET response was observed (Fig. 2b), although substantial phosphorylation of Y580 occurred (Supplementary Fig. S1e). Since the only difference between Δ580 and Δ542 reporters is their distinct sequences at position 542 (Fig. 2a,b), the stronger FRET response of Δ580 reporter with pY542 sequence confirms that C-SH2 also favors the pY542 sequence over pY580 in the context of the whole Shp2 protein. The dominant *cis*-interaction between pY580 and C-SH2 within the WT reporter where both Y542 and Y580 are phosphorylated, therefore, suggests that position 580 may be favored over position 542 for C-SH2 interaction to overpower the advantageous pY542 sequence. Indeed, when the reporter was reengineered to have identical Y542 sequence at both 542 and 580 positions (Y542Y542), position 580 is the preferred *cis*-interaction site for C-SH2 because a mutation at position 580 but not 542 suppressed the majority of FRET response (Fig. 2d). Therefore, the dominant *cis*-interaction between C-SH2 and pY580 within the WT reporter *in vitro* is resulted from an antagonistic combination of an adverse sequence but a favorable position at pY580.

Different conformational regulation of Shp2 in cells

Both purified WT reporter and full-length Shp2 *in vitro* showed an increased phosphatase activity upon incubation with PDGFRβ, which can interact with the N-SH2 domain and therefore unmask the phosphatase domain to activate Shp2 (Supplementary Fig. S2a). When expressed in mouse embryonic fibroblasts (MEFs), the WT reporter was recruited to membrane ruffles after platelet-derived growth factor (PDGF) stimulation with similar localization and C-tail phosphorylation as the endogenous Shp2 (Supplementary Fig. S2b,c). Therefore, the Shp2 reporter has the same functional activation mechanism and localizations as the endogenous Shp2. We hence applied the Shp2 reporter to monitor Shp2 conformation regulations in mammalian cells. We confirmed that the cellular concentration of Shp2 reporter when expressed in mammalian cells to be in the range of micro molar, which is similar to the concentration used *in vitro* (Supplementary Fig. S2d). PDGF caused a FRET increase of the WT reporter in MEFs (Fig. 3a, Supplementary Fig. S3a, and Supplementary Movie 1), concomitant with phosphorylation at both Y542 and Y580 (Supplementary Fig. S2c). In contrast, no FRET response can be observed upon PDGF stimulation in MEFs expressing both ECFP-Shp2 and Shp2-YPet (Supplementary Fig. S3b), confirming the *cis*-interaction within WT reporter for the FRET change in live cells. Consistent with our *in vitro* results, RDL, YDF, or R138L, but not R32L mutation, abolished the FRET response (Fig. 3b, Supplementary Fig. S3c). Surprisingly, in marked contrast to their effects *in vitro*, Y542F but not Y580F mutation, eliminated the PDGF-induced FRET response in MEFs (Fig. 3b, Supplementary Fig. S3c, Supplementary Movie 2 and 3). The *cis*-interaction

Author Manuscript Author Manuscript Author Manuscript Author Manuscript

between pY542 and C-SH2 is hence dominant in MEFs, in contrast to the pY580 and C-SH2 pair *in vitro*. Consistently, the Y580F reporter, with its Y542 intact and phosphorylated (Fig. 3c), had a similar level of FRET change as that of WT reporter in MEFs (Fig. 3b). The Δ580 reporter also had stronger FRET responses than the WT reporter in MEFs, which was abolished by additional R138L but not R32L mutation (Supplementary Fig. S3d). All these results confirmed the primary *cis*-interaction between pY542 and C-SH2 in MEFs.

Y580 phosphorylation depends on Y542 and C-SH2 in MEFs

We further explored the molecular mechanism underlying the distinct conformational regulations of Shp2 *in vitro* and in MEFs. Y580 phosphorylation in the absence of Y542 was significantly inhibited in MEFs (Fig. 3c) [22], in contrast to the independence of Y580 and Y542 phosphorylations *in vitro* (Fig. 1g). The phosphorylation of Y542 is hence essential for and may occur prior to pY580 within each copy of the reporters in MEFs. Indeed, Y542 sequence fused to GFP was phosphorylated substantially faster than Y580 sequence *in vitro* (Fig. 3d). R138L mutant to disrupt C-SH2 also inhibited the phosphorylation of Y580, but not that of Y542 in MEFs (Fig. 3e). Hence, pY542 and its subsequent *cis*-interaction with C-SH2 can precede and mediate the phosphorylation of Y580 in MEFs.

Grb2 tunes *cis*-interactions and FRET levels of Shp2 reporter

We then examined whether the phosphorylation of Y580, in the absence of pY542, can be rescued in MEFs to allow its *cis*-interaction with C-SH2 as it does *in vitro*. When PDGFRβ was overexpressed in MEFs, Y580 phosphorylation can occur in the absence of pY542 (Fig. 4a) to cause C-SH2/pY580 interaction and result in a considerable FRET change upon PDGF stimulation (Fig. 4b). It was puzzling then why the C-SH2/pY580 *cis*-interaction dominates *in vitro* but not in MEFs when both Y542 and Y580 are phosphorylated in the WT reporter. Because the phosphorylation of Y580 follows and is dependent on the *cis*-interaction of C-SH2/pY542 in MEFs, we hypothesized that molecules interacting with Shp2 in MEFs, such as Grb2 [23], may sequester the more potent pY580 from competing for the pY542-occupied C-SH2. Indeed, purified Grb2 can reduce and tune the FRET levels when added to the phosphorylated Y542F reporter *in vitro* (Fig. 4c), by interacting with the available pY580 in the reporter (Fig. 4d). The amount of Grb2 can apparently cause a proportional reduction in overall FRET signals by decreasing the percentage of reporters adopting high-FRET *cis*-interactions (Fig. 4c,d). This tuning ability of Grb2 is mediated by its SH2 domain as the SH2-disabling mutant Grb2RV was no longer effective (Fig. 4e). Consistently, overexpression of Grb2 with varying concentrations can proportionally tune, via its SH2 domain, the FRET level of the Y542F reporter in MEFs overexpressing constitutively active PDGFR (Tel-PDGFRβ) [24] (Fig. 5a,b). Therefore, Grb2 can *trans*-interact with and sequester pY580 from *cis*-interaction with C-SH2 in Y542F reporter. Further results showed that Grb2 can also tune the FRET signals of WT reporter in MEFs (Fig. 5c). However, it is unclear whether Grb2 preferentially *trans*-interacts with pY580 when both Y542 and Y580 are intact and phosphorylated in the WT reporter. SPR results revealed that Grb2 has a significantly higher affinity binding to the isolated pY580 peptide than to the pY542 peptide (Table 1). In addition, R138L mutation disrupting the C-SH2 occupation of pY542 in the Y580F reporter significantly increased the pY542-Grb2 interaction (Fig. 5d), suggesting that the pre-formed *cis*-interaction of C-SH2 and pY542 can

Author Manuscript Author Manuscript Author Manuscript Author Manuscript

reduce the availability of pY542 for Grb2 and hence promote Grb2-pY580 interaction in the WT reporter. Indeed, pY542 in the Y580F reporter allowed much less Grb2 binding comparing to the WT reporter (Fig. 5e), confirming that pY580 in Shp2 is the preferred and primary *trans*-interaction site for Grb2. This Grb2-pY580 association can sequester the free pY580 from competing for the pY542-occupied C-SH2, which should in turn stabilize the pY542/C-SH2 complex in MEFs (Fig. 5f).

Rewired Shp2 reprograms *cis*-interaction and ERK dynamics

Based on the results, it is clear that the Y542 contextual sequence is favored as a substrate for PDGFR and has a higher affinity for C-SH2 upon phosphorylation. However, position 580 is favored by C-SH2 for the *cis*-interaction over position 542 within the context of the intact Shp2 molecule. This antagonistic combination of sequence and position results in a favored *cis*-interaction between C-SH2 and Y580 *in vitro*, where both Y542 and Y580 are independently phosphorylated by the PDGFR in solution. In MEFs, the recruitment of Shp2 to the membrane receptor PDGFR through its N-SH2 domain[25] leads to an early phosphorylation of the favored substrate Y542, which subsequently undergoes *cis*-interaction with C-SH2. This pY542/C-SH2 interaction and the resulted conformational change are essential and facilitate the phosphorylation of Y580, which recruits Grb2 to sequester the otherwise favored pY580 from competing for the pY542-occupied C-SH2. As such, Grb2 in MEFs can bind to pY580 and shift the equilibrium of *cis*-interaction toward pY542/C-SH2, distinct from the dominant pY580/C-SH2 *cis*-interaction of Shp2 in solutions.

It hence becomes apparent that the moderate difference between pY542 and pY580 in competing for C-SH2, resulting from the antagonistic combination of tyrosine sequence and position, can allow easier alteration of Shp2 *cis*-interactions by Grb2 binding. We have then rewired the modular arrangement within Shp2 to develop a SWAP reporter by swapping the Y542 and Y580 sequences to combine the favorable Y542 sequence with the preferred 580 position in a synergistic fashion (Y542’: Y580 sequence at 542 position; Y580’: Y542 sequence at 580 position), widening the gap of competitiveness between the two tyrosines (Fig. 6a).

We thereafter examined the characteristics of the SWAP reporter *in vitro* and in MEFs. Y542’ and Y580’ of the SWAP reporter were phosphorylated independently both *in vitro* and in MEFs (Fig. 6b). PDGF also induced a remarkably high FRET change of the SWAP reporter in MEFs, significantly stronger than that of the WT reporter and with a level as high as the *in vitro* response (Supplementary Fig. S4a,b; Fig. 3b, Supplementary Movie 4). More importantly, Y580’F or R138L, but not Y542’F nor R32L, abolished the FRET response of the SWAP reporter both *in vitro* and in MEFs (Fig. 6c,d; Supplementary Fig. S4c,d; Supplementary Movie 5 and 6). These results confirmed that the SWAP reporter loses the tunable *cis*-interactions with its C-SH2 and undergoes one form of *cis*-interaction with the pY580’ and C-SH2 pair both *in vitro* and in MEFs. The Y542’ phosphorylation of SWAP reporter was also lower than that of WT reporter (Supplementary Fig. S4e), suggesting that the regulatory mechanism of promoting Y580 phosphorylation by C-SH2/pY542 *cis*-interaction no longer exists in the SWAP reporter. Consequently, this rewired *cis*-regulation

Author Manuscript Author Manuscript Author Manuscript Author Manuscript

of Shp2 conformation caused a significantly more transient ERK phosphorylation upon PDGF stimulation (Fig. 6e, Supplementary Fig. S4f). Therefore, by swapping the Y542 and Y580 sequences, we have rewired the regulation mechanism of Shp2 conformation, which led to a reprogrammed downstream ERK signaling.

DISCUSSION

Our results indicate that a simple antagonistic combination of contextual sequence and position can result in tunable *cis*-interactions within Shp2, leading to complex regulation routes and functional outcomes. pY542 in the WT reporter has the combination of favored sequence and adverse position while pY580 has adverse sequence and favored position. Swapping the sequences results in a synergistic combination: pY580' with favored sequence and position while pY542' with adverse sequence and position (Fig. 6a). As such, the order of these four phosphotyrosines in terms of their affinity for C-SH2 is as follows: pY542' < pY542 < pY580 < pY580'. Therefore, the antagonistic combination has two layers of effect on the *cis*-interactions of Shp2. First, it ensures that the affinity of bothpY542 and pY580 in WT Shp2 for *cis*-regulation is moderate enough to allow effective *trans*-regulations and prevent possibly insurmountable *cis*-interactions as in the case of pY580'. This note is supported by the observation that Grb2 more effectively inhibit the FRET response of Y542 reporter (pY580 and C-SH2 *cis*-interaction) than that of Y542'FSWAP (pY580' and C-SH2 *cis*-interaction) (Supplementary Fig. S5a). In addition, the affinity of Grb2 toward isolated pY542 or pY580 peptide is several orders higher than that of C-SH2 (Table 1). This higher affinity of Grb2 allows the effective competitiveness of *trans*-interaction, overcoming the entropic advantage of *cis*-interactions with the WT Shp2 [26]. Second, the antagonistic combination can lead to a relatively small difference in the *cis*-interaction competitiveness between the two phosphotyrosines than the synergistic combination (pY580 - pY542 < pY580' - pY542'). Therefore, the presence of Grb2 in mammalian cells can tune the *cis*-interaction of WT Shp2 toward pY542/C-SH2 pair from pY580/C-SH2 pair. In contrast, the pY580'/C-SH2 pair in SWAP reporter dominates both in cells and *in vitro*. As such, the synergistic combination in the SWAP reporter resulted in the enlargement of the difference in competitiveness between the two phosphotyrosines, the inhibition of Grb2-mediated *trans*-regulation, the loss of tunable *cis*-interactions within Shp2, and eventually the reprogramming of downstream ERK signaling dynamics. This combinatorial effect of protein modules is strikingly similar to that of DNA *cis*-regulatory elements on regulating a coordinated gene expression where sequence-specific promoters/enhancers are highly structured and precisely positioned [4,5,27]. We suggest that this antagonistic combination of protein sequence and position can serve as a basic design principle for the construction of tunable protein elements and building blocks to develop higher order and programmable molecular machineries, capable of learning and adapting according to environmental cues.

Systems and synthetic biologists have long employed networks to describe the signaling transduction, with each node representing one molecule and its determined function [28]. We discovered in this work that a tunable regulation mechanism is embedded within one molecule, for the processing of environmental inputs to result in differential Shp2 conformations and functional outcomes. These *cis*-interactions within Shp2 allow the fine regulation of protein functions beyond the simple disruption of autoinhibition for protein

Author Manuscript Author Manuscript Author Manuscript Author Manuscript

activations. This protein-based regulation can also produce fast responses at specific subcellular locations, surpassing the capacity of gene-based tuning of cellular functions [29]. Hence, this tunable regulation mechanism built in Shp2 may provide a prominent example on how nature can design/evolve molecules with their conformations/functions differentially regulated under different subcellular environments. Integrating with molecular switches/gates based on scaffold proteins [30,31] and genetic circuits [29], the understanding and rewiring of these modular motif arrangements may also provide powerful means to reprogram the downstream signaling cascades at subcellular levels [28]. It is of note that this tunable *cis*-interactions within Shp2 may not exist in lower organisms since the *Drosophila* ortholog, Corkscrew, only retains Y542 while the *Caenorhabditis. elegans* ortholog, Ptp-2, lacks both tyrosines [18]. Therefore, this *cis*-regulatory mechanism of Shp2 may represent a distinguished evolutionary innovation in higher organisms for the fine-tuning of functions resulting in higher levels of organism complexity [32]. In addition, our results only show that Grb2 can tune the *cis*-interaction of Shp2. However, Grb2 may not be the only molecule that can *trans*-regulate Shp2 function, as Grb2 siRNA knockdown didn't decrease the FRET level of Y542F reporter compared to control siRNA (Supplementary Fig. S5b).

Our FRET-based Shp2 reporter mainly revealed the *cis*-interactions between phosphotyrosines and C-SH2, but not N-SH2. It appears unlikely that N-SH2 has *cis*-interactions with pY542 or pY580 since the binding cleft of N-SH2 domain in the full-length Shp2 is in a compressed and closed conformation limiting accessibility for phosphopeptides [33,34]. It has been established that the phosphotyrosine interaction of N-SH2 can drastically affect the Shp2 phosphatase activity by relieving the autoinhibitory *cis*-interaction between N-SH2 and PTP domain [35,36]. In our study, the binding of C-SH2 by either pY542 or pY580 did not have significant impact on the phosphatase activity since the phosphatase activity of R32L reporter did not increase after being phosphorylated by PDGFR kinase (Supplementary Fig. S5c,d). Therefore, the SH2 domain interactions within Shp2 can have two main functional outcomes: the *trans*-interaction of N-SH2 regulates phosphatase enzymatic activity whereas that *cis*-interaction of C-SH2 controls the Y580 phosphorylation and the subsequent Grb2 recruitment to govern downstream signaling cascades, such as ERK phosphorylation.

While the initial phosphorylation of ERK is mainly dependent on the receptor-Ras pathway [37], the phosphorylation of Y580 is crucial for the maintenance of a sustained ERK phosphorylation [22]. Indeed, it has been proposed that pY580 may serve as a docking site for Grb2/Sos complex and therefore regulate downstream ERK pathway [38]. In the SWAP reporter, pY542' was also constitutively lower (Supplementary Fig. S4e), causing a transient ERK phosphorylation (Fig. 6e). Since the different dynamics of ERK activation has been shown to determine cell fate and long-term memory [39,40], the wiring and re-wiring of Y542 and Y580 positions in Shp2 to control pY580/pY542' and hence ERK phosphorylation dynamics can have profound impact on pathophysiological consequences.

The modular SH2-phosphotyrosine *trans*-interaction between different proteins has been well established to mediate molecular interactions and signaling transduction[41]. The intramolecular *cis*-interaction of SH2-phosphotyrosine has also been shown to regulate the molecular functions[42]. For example, the *cis*-interaction between pY527 and SH2 domain of

Author Manuscript Author Manuscript Author Manuscript Author Manuscript

Src kinase can cause the auto-inhibition of Src kinase domain[43]. The SH2-phosphotyrosine *trans*-interaction can further compete for the *cis*-interaction of domains within a molecule and modulate the molecular function. Indeed, Src SH2 domain can interact with pY397 at FAK to release the FERM domain from masking the FAK kinase domain and cause FAK activation[44]. However, most studies involve only one pair of SH2-phosphotyrosine interaction. The Shp2 molecule has two coordinating pairs of SH2-phosphotyrosine interaction. Our results suggest that an antagonistic combination of sequence and position of the phosphorylated tyrosines can result in tunable *cis*-interactions within one molecule to allow effective *trans*-regulations of its conformational changes and subsequently functions. With the prevalence of SH2-phosphotyrosine and other modules, the complexity revealed by our FRET-based study of *cis*-interactions between multiple interacting domains may be a typical but overlooked layer that contributes to the overall complexity of cell signaling.

METHODS

Reporter construction and other constructs

The Shp2 reporter was constructed by fusing a full length human Shp2 cDNA to an N-terminal ECFP sequence and a C-terminal YPet sequence in pRSETb (Invitrogen) for bacterial expression. For mammalian cell expression, the Shp2 reporter was cloned into pcDNA3.1 (Invitrogen) behind a Kozak sequence using BamHI/EcoRI restriction sites. Point mutations of the Shp2 reporters were generated using QuikChange Site-Directed Mutagenesis Kit (Stratagene). Deletion or insertion mutations of Shp2 reporter were generated by PCR and subsequent ligation. The sequence of 11 amino acids surrounding Y542 or Y580 (including 4 residues in front of and 6 residues behind tyrosine) was referred as Y542 or Y580 sequence, respectively. The Δ542 reporter has a truncation between residue 538 and 575 whereas the Δ580 reporter has a truncation between residue 556 and 593. The SWAP reporter has the 11 aa sequences surrounding Y542 and Y580 exchanged. The Y542Y542 reporter has the Y542 sequence at both Y542 and Y580 positions. Tel-PDGFRβ constructs were from Dr. Gary Gilliland.

Protein expression and purification

HEK cells (ATCC) transfected with WT or mutated Shp2 reporters were washed with cold PBS and then lysed in buffer containing 50 mM Tris-HCl pH 7.5, 100 mM NaCl, 1 mM EDTA, 0.2 mM PMSF, 0.2% Triton X-100 and a protease inhibitor cocktail tablet (Roche). Lysates were centrifuged at 10,000 x g at 4°C for 10 min. Supernatants were incubated with Ni-NTA agarose beads (Qiagen), which were then washed with 50 mM Tris-HCl pH 7.5, 100 mM NaCl, 10 mM imidazole. Reporter proteins were eluted in a buffer containing 50 mM Tris-HCl pH 7.5, 100 mM NaCl, and 100 mM imidazole. Alternatively, reporter proteins were purified from E. coli for large quantities. Reporters in pRSETb were transformed into BL21 and the expression was induced by exposure to 0.4 mM IPTG for 16 hr at room temperature. The bacteria were lysed in buffer A (20 mM imidazole, 20 mM Tris-HCl pH 8, 200 mM NaCl) with EmulsiFelx-B15 (Avestin). Lysates were centrifuged at 10,000 x g at 4°C for 20 min. Supernatants were then loaded onto a HisTrap HP column using an AKTA purifier FPLC system (GE). The column was subsequently washed with 20 ml of buffer A and the fusion protein eluted using a 20–400 mM imidazole concentration

Author Manuscript Author Manuscript Author Manuscript Author Manuscript

gradient developed in 50 ml buffer A at 0.5 ml/min. Fractions with absorption at 430 nm were pooled, concentrated and subsequently loaded onto a HiLoad 16/60 Superdex 200 gel filtration column (GE). Buffer B (30 mM Tris-HCl pH 8.0, 200 mM NaCl, 1 mM dithiothreitol) was then used for elution. Fractions around MW 120 kDa were collected and concentrated for *in vitro* assays.

Immunoprecipitation (IP) and immunoblotting (IB)

Cells were washed three times with ice-cold PBS and lysed in a buffer (Cell Signaling) containing 50 mM Tris-HCl, pH 7.5, 125 mM NaCl, 1% Triton X-100, 0.1% SDS, 5 mM NaF, 1 mM Na3VO4, 1 mM phenylmethylsulfonyl fluoride, and 10 μg/ml leupeptin. Lysates were centrifuged at 10,000 x g at 4°C for 10 min, and the protein concentration of clarified lysates was determined by Bradford assay (Biorad). Antibodies (1μg/100 μg total lysate) for Co-IP or IP were incubated with cell lysates for 1 hr at 4°C. Protein A/G beads (Santa Cruz) were then added to the mixture and incubated overnight at 4°C. The beads were washed three times with lysis buffer and boiled for 5 min in SDS protein loading buffer. After centrifugation, the supernatants were resolved by SDS-PAGE. The proteins were then transferred onto a nitrocellulose membrane and blocked with 5% bovine serum albumin in TTBS buffer (50 mM Tris-HCl, 145 mM NaCl, 0.05% Tween-20, pH 7.4) for 2 hr at room temperature (RT). Membranes were further incubated with primary antibodies overnight at 4°C, washed and then incubated with HRP-conjugated secondary antibodies for 2 hr at RT. Signals were detected using SuperSignal Western Pico or Femto ECL Kit (Pierce). Western results were quantified with ImageJ (NIH). Our statistics were performed with two-tailed Student t-test. When multiple t-tests were performed, the α-value was modified by the Bonferroni correction, such that α=0.0125 for up to four t-tests performed in each group (Fig. 5). Anti-phospho-SHP-2 (Tyr-542) and (Tyr-580) antibodies were from Cell Signaling Technology (Cat # 3751 and 3703). Anti-GFP antibody for IP was from Abcam (Cat # ab290). Anti-phosphotyrosine pY20 antibody was from BD Transduction laboratory (Cat # 610000). Anti-Shp2, anti-GFP antibodies for immunoblotting as well as HRP-conjugated secondary antibodies were purchased from Santa Cruz Biotechnology (Cat # sc-280, sc-8334, sc-2004, sc-2005).

Image acquisition and analysis

Glass-bottom dishes (Cell E&G Inc.) were coated with 10 μg/ml fibronectin (Sigma) overnight at 37°C. Transfected MEFs were plated onto these dishes overnight in DMEM containing 0.5% FBS before imaging. During imaging, MEFs (ATCC) were maintained in CO2-independent medium (Invitrogen) with 0.5% FBS at 37°C for 10 min before treatment with 20 ng/ml PDGF (Sigma). Images were obtained on a Zeiss Axiovert inverted microscope equipped with a cooled charge-coupled device camera (Cascade 512B; Photometrics) using MetaFluor 6.2 software (Universal Imaging). The following filter sets (Chroma) were used in our experiments for FRET imaging: a dichroic mirror (450 nm), an excitation filter 420/20 nm, an ECFP emission filter 475/40 nm, and a FRET emission filter 535/25 nm. The excitation filter for ECFP at 420±20 nm was specifically selected to shift toward lower wavelength away from the peak excitation spectrum of ECFP to reduce the cross-excitation of the FRET acceptor YPet which has significantly higher brightness than ECFP. This filter selection can minimize the effect of bleed-through on the FRET channel.

Author Manuscript Author Manuscript Author Manuscript Author Manuscript

The fluorescence intensity of non-transfected cells was quantified as the background signal and subtracted from the ECFP and FRET signals of transfected cells. The pixel-by-pixel ratio images of FRET/ECFP were calculated based on the background-subtracted fluorescence intensity images of ECFP and FRET by using the MetaFluor software. These ratio images were displayed in the intensity modified display mode in which the color and brightness of each pixel is determined by the FRET/ECFP ratio and ECFP intensity, respectively. The emission ratio were quantified and analyzed by Excel (Microsoft).

In vitro kinase assays

Purified proteins were dialyzed overnight at 4°C in kinase buffer (50 mM Tris-HCl pH 8.0, 100 mM NaCl, 10 mM MgCl2, and 2 mM dithiothreitol). Fluorescence emission spectra of the purified reporters (0.5 μM) were measured in 96-well plates with an excitation wavelength of 430 nm using a fluorescence plate reader (TECAN, Sapphire II). Emission ratios of acceptor/donor (526 nm/478 nm) were measured at 30°C before and after the addition of 1 mM ATP and 10-100 nM active PDGFRβ kinases (Millipore).

Affinity measurement by SPR

The binding affinity of pY542 and pY580 peptides to C-SH2 domain or Grb2 was assessed by SPR analysis on a BIAcore 3000 instrument (GE). Biotinylated peptides were immobilized on streptavidin-coated SA sensor chips (GE). Prior to immobilization, the sensor chip was conditioned with a solution containing 1 M NaCl and 50 mM NaOH. The binding assay were conducted at room temperature in HBS-EP buffer (GE, 10 mM HEPES, pH 7.4, 150 mM NaCl, 3 mM EDTA, 0.005% Surfactant P20). Each pY peptide was injected at a flow rate of 5 μl/min until a constant level of response units (500–600 RU) was obtained. Varying concentrations of histidine-tagged C-SH2 or Grb2 were passed over the immobilized peptides for 2 min. To remove the proteins from the peptide, a regeneration buffer (10 mM NaOH, 200 mM NaCl, 0.05% SDS) was applied. The equilibrium response unit (RUeq) at a given protein concentration was obtained by subtracting the response of a blank control chip. The dissociation constants (Kd) were calculated by the BIAevaluation software using the equation 1, where RUeq is the measured response unit at a given SH2 domain concentration, and RUmax is the maximum response unit:

$$RUeq = RUmax\ [SH2] / (Kd + [SH2]) \quad \text{(Eq. 1)}$$

Immunostaining

Cells were washed three times with ice-cold PBS and fixed with 4% paraformaldehyde at RT for 15 min before they were permeabilized with 0.1% TritonX-100 in PBS for 30 min. After that, the cells were rinsed and blocked with 1% BSA in PBS for 20 min. They were then incubated with primary antibody (Santa Cruz, Cat # sc-280 or sc-8994, 1:1000 dilution) in PBS at RT for 2 hr before they were incubated with secondary antibody conjugated with fluorescence dye at RT for 1 hr. After another round of washing, the cells were subjected to imaging under microscopy.

Author Manuscript Author Manuscript Author Manuscript Author Manuscript

Phosphatase activity assays

Phosphatase activity was measured using fluorogenic 6,8-difluoro-4-methylumbelliferyl phosphate (DiFMUP; Invitrogen) as the substrate. Each reaction contained 50 mM Tris pH 8, 100 mM NaCl, 10 mM MgCl2, 2mM dithiothreitol, 20 μM DiFMUP, and 20 nM Shp2 reporter in a total reaction volume of 100 μl in a well of 96-well plates. Reactions were initiated by the addition of DiFMUP, followed by incubation for 30 min at 30°C. The fluorescence signal of the reaction product, 6,8-difluoro-4-methylumbelliferone, was measured at an excitation wavelength of 355 nm and an emission of 460 nm with a plate reader.

Supplementary Material

Refer to Web version on PubMed Central for supplementary material.

Acknowledgments

We thank Professor Gary Gilliland (Harvard University) for the Tel-PDGFRβ construct. This work is supported by grants from NIH HL098472, CA139272, NSF CBET0846429 (Y.W.) and NIH R37 CA49132, the Ontario Ministry of Health and Long Term Care, and the Princess Margaret Hospital Foundation (B.G.N.).

Abbreviations

FRET	fluorescence resonance energy transfer
FP	fluorescence protein
ECFP	enhanced cyan fluorescence protein
YPet	YFP for energy transfer
PDGF	platelet-derived growth factor
MEF	mouse embryonic fibroblast
Shp2	Src homology 2 (SH2) domain-containing protein tyrosine phosphatase 2

References

1. Pufall MA, Graves BJ. Autoinhibitory domains: modular effectors of cellular regulation. Annu Rev Cell Dev Biol. 2002; 18:421–462. [PubMed: 12142282]
2. Bhattacharyya RP, Remenyi A, Yeh BJ, Lim WA. Domains, motifs, and scaffolds: the role of modular interactions in the evolution and wiring of cell signaling circuits. Annu Rev Biochem. 2006; 75:655–680. [PubMed: 16756506]
3. Woody ST, Fong RS, Gussin GN. Effects of a single base-pair deletion in the bacteriophage lambda PRM promoter. Repression of PRM by repressor bound at OR2 and by RNA polymerase bound at PR. J Mol Biol. 1993; 229:37–51. [PubMed: 8421315]
4. Cox RS 3rd, Surette MG, Elowitz MB. Programming gene expression with combinatorial promoters. Mol Syst Biol. 2007; 3:145. [PubMed: 18004278]
5. Murphy KF, Balazsi G, Collins JJ. Combinatorial promoter design for engineering noisy gene expression. Proc Natl Acad Sci U S A. 2007; 104:12726–12731. [PubMed: 17652177]
6. Sakon JJ, Weninger KR. Detecting the conformation of individual proteins in live cells. Nat Methods. 2010; 7:203–205. [PubMed: 20118931]

Author Manuscript Author Manuscript Author Manuscript Author Manuscript

7. Kiyokawa E, Hara S, Nakamura T, Matsuda M. Fluorescence (Forster) resonance energy transfer imaging of oncogene activity in living cells. Cancer Sci. 2006; 97:8–15. [PubMed: 16367915]
8. Wang Y, Shyy JY, Chien S. Fluorescence proteins, live-cell imaging, and mechanobiology: seeing is believing. Annu Rev Biomed Eng. 2008; 10:1–38. [PubMed: 18647110]
9. Aye-Han NN, Ni Q, Zhang J. Fluorescent biosensors for real-time tracking of post-translational modification dynamics. Curr Opin Chem Biol. 2009; 13:392–397. [PubMed: 19682946]
10. Lam AJ, et al. Improving FRET dynamic range with bright green and red fluorescent proteins. Nat Methods. 2012; 9:1005–1012. [PubMed: 22961245]
11. Tonks NK. Protein tyrosine phosphatases: from genes, to function, to disease. Nat Rev Mol Cell Biol. 2006; 7:833–846. [PubMed: 17057753]
12. Bard-Chapeau EA, et al. Ptpn11/Shp2 acts as a tumor suppressor in hepatocellular carcinogenesis. Cancer Cell. 2011; 19:629–639. [PubMed: 21575863]
13. Chan G, Kalaitzidis D, Neel BG. The tyrosine phosphatase Shp2 (PTPN11) in cancer. Cancer Metastasis Rev. 2008; 27:179–192. [PubMed: 18286234]
14. Tartaglia M, et al. Mutations in PTPN11, encoding the protein tyrosine phosphatase SHP-2, cause Noonan syndrome. Nat Genet. 2001; 29:465–468. [PubMed: 11704759]
15. Tartaglia M, Gelb BD. Noonan syndrome and related disorders: genetics and pathogenesis. Annu Rev Genomics Hum Genet. 2005; 6:45–68. [PubMed: 16124853]
16. Loh ML, et al. Mutations in PTPN11 implicate the SHP-2 phosphatase in leukemogenesis. Blood. 2004; 103:2325–2331. [PubMed: 14644997]
17. Tartaglia M, et al. Somatic mutations in PTPN11 in juvenile myelomonocytic leukemia, myelodysplastic syndromes and acute myeloid leukemia. Nat Genet. 2003; 34:148–150. [PubMed: 12717436]
18. Neel BG, Gu H, Pao L. The 'Shp'ing news: SH2 domain-containing tyrosine phosphatases in cell signaling. Trends Biochem Sci. 2003; 28:284–293. [PubMed: 12826400]
19. Lu W, Gong D, Bar-Sagi D, Cole PA. Site-specific incorporation of a phosphotyrosine mimetic reveals a role for tyrosine phosphorylation of SHP-2 in cell signaling. Mol Cell. 2001; 8:759–769. [PubMed: 11684012]
20. Ouyang M, Sun J, Chien S, Wang Y. Determination of hierarchical relationship of Src and Rac at subcellular locations with FRET biosensors. Proc Natl Acad Sci U S A. 2008; 105:14353–14358. [PubMed: 18799748]
21. Eck MJ, Pluskey S, Trub T, Harrison SC, Shoelson SE. Spatial constraints on the recognition of phosphoproteins by the tandem SH2 domains of the phosphatase SH-PTP2. Nature. 1996; 379:277–280. [PubMed: 8538796]
22. Araki T, Nawa H, Neel BG. Tyrosyl phosphorylation of Shp2 is required for normal ERK activation in response to some, but not all, growth factors. J Biol Chem. 2003; 278:41677–41684. [PubMed: 12923167]
23. Li W, et al. A new function for a phosphotyrosine phosphatase: linking GRB2-Sos to a receptor tyrosine kinase. Mol Cell Biol. 1994; 14:509–517. [PubMed: 8264620]
24. Carroll M, Tomasson MH, Barker GF, Golub TR, Gilliland DG. The TEL/platelet-derived growth factor beta receptor (PDGF beta R) fusion in chronic myelomonocytic leukemia is a transforming protein that self-associates and activates PDGF beta R kinase-dependent signaling pathways. Proc Natl Acad Sci U S A. 1996; 93:14845–14850. [PubMed: 8962143]
25. Nakata S, et al. Regulation of platelet-derived growth factor receptor activation by afadin through SHP-2: implications for cellular morphology. J Biol Chem. 2007; 282:37815–37825. [PubMed: 17971444]
26. Nguyen JT, Lim WA. How Src exercises self-restraint. Nat Struct Biol. 1997; 4:256–260. [PubMed: 9095189]
27. Levine M, Tjian R. Transcription regulation and animal diversity. Nature. 2003; 424:147–151. [PubMed: 12853946]
28. Lim WA. Designing customized cell signalling circuits. Nat Rev Mol Cell Biol. 2010; 11:393–403. [PubMed: 20485291]

Author Manuscript Author Manuscript Author Manuscript Author Manuscript

29. Lu TK, Khalil AS, Collins JJ. Next-generation synthetic gene networks. Nat Biotechnol. 2009; 27:1139–1150. [PubMed: 20010597]
30. Bashor CJ, Helman NC, Yan S, Lim WA. Using engineered scaffold interactions to reshape MAP kinase pathway signaling dynamics. Science. 2008; 319:1539–1543. [PubMed: 18339942]
31. Good MC, Zalatan JG, Lim WA. Scaffold proteins: hubs for controlling the flow of cellular information. Science. 2011; 332:680–686. [PubMed: 21551057]
32. Lim WA, Pawson T. Phosphotyrosine signaling: evolving a new cellular communication system. Cell. 2011; 142:661–667. [PubMed: 20813250]
33. Darian E, Guvench O, Yu B, Qu CK, MacKerell AD Jr. Structural mechanism associated with domain opening in gain-of-function mutations in SHP2 phosphatase. Proteins. 2011; 79:1573–1588.10.1002/prot.22984 [PubMed: 21365683]
34. Guvench O, Qu CK, MacKerell AD Jr. Tyr66 acts as a conformational switch in the closed-to-open transition of the SHP-2 N-SH2-domain phosphotyrosine-peptide binding cleft. BMC structural biology. 2007; 7:14.10.1186/1472-6807-7-14 [PubMed: 17378938]
35. Sugimoto S, Wandless TJ, Shoelson SE, Neel BG, Walsh CT. Activation of the SH2-containing protein tyrosine phosphatase, SH-PTP2, by phosphotyrosine-containing peptides derived from insulin receptor substrate-1. J Biol Chem. 1994; 269:13614–13622. [PubMed: 7513703]
36. Hof P, Pluskey S, Dhe-Paganon S, Eck MJ, Shoelson SE. Crystal structure of the tyrosine phosphatase SHP-2. Cell. 1998; 92:441–450. [PubMed: 9491886]
37. Egan SE, et al. Association of Sos Ras exchange protein with Grb2 is implicated in tyrosine kinase signal transduction and transformation. Nature. 1993; 363:45–51. [PubMed: 8479536]
38. Dance M, Montagner A, Salles JP, Yart A, Raynal P. The molecular functions of Shp2 in the Ras/Mitogen-activated protein kinase (ERK1/2) pathway. Cell Signal. 2008; 20:453–459. [PubMed: 17993263]
39. Santos SD, Verveer PJ, Bastiaens PI. Growth factor-induced MAPK network topology shapes Erk response determining PC-12 cell fate. Nat Cell Biol. 2007; 9:324–330. [PubMed: 17310240]
40. Pagani MR, Oishi K, Gelb BD, Zhong Y. The phosphatase SHP2 regulates the spacing effect for long-term memory induction. Cell. 2009; 139:186–198. [PubMed: 19804763]
41. Pawson T, Gish GD, Nash P. SH2 domains, interaction modules and cellular wiring. Trends in cell biology. 2001; 11:504–511. [PubMed: 11719057]
42. Boggon TJ, Eck MJ. Structure and regulation of Src family kinases. Oncogene. 2004; 23:7918–7927. [PubMed: 15489910]
43. Brown MT, Cooper JA. Regulation, substrates and functions of src. Biochimica et biophysica acta. 1996; 1287:121–149. [PubMed: 8672527]
44. Mitra SK, Hanson DA, Schlaepfer DD. Focal adhesion kinase: in command and control of cell motility. Nat Rev Mol Cell Biol. 2005; 6:56–68.10.1038/nrm1549 [PubMed: 15688067]

Author Manuscript Author Manuscript Author Manuscript Author Manuscript

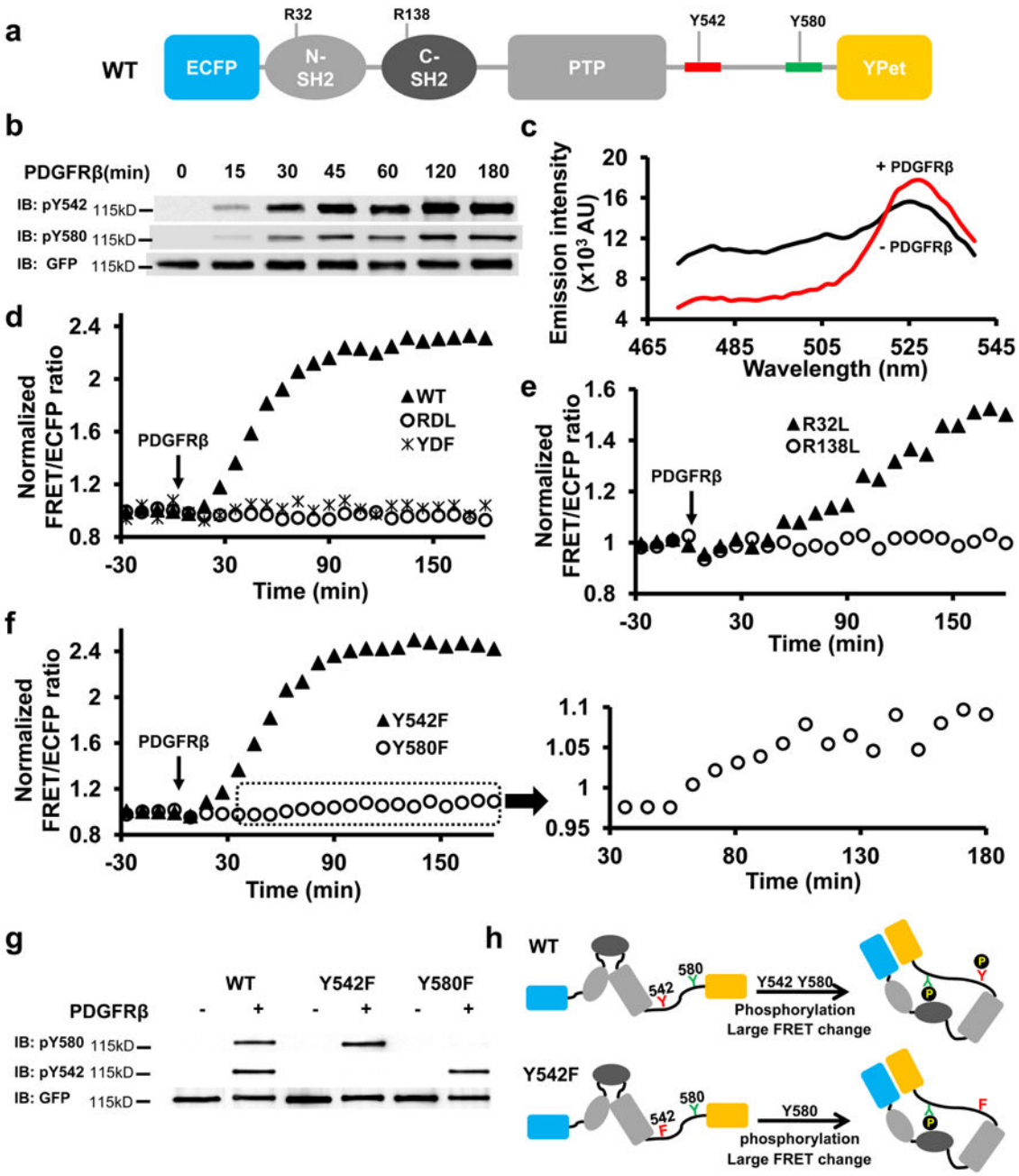

Figure 1. *cis*-Interactions of the Shp2 reporters *in vitro*

(**a**) Schematic drawing of the WT Shp2 reporter, with mutation sites as indicated. Y542 and Y580 sequences are colored in red and green, respectively. (**b**) The phosphorylation of WT reporter upon PDGFRβ incubation *in vitro*(refer to Supplementary Figure S6a for the whole blots). (**c**) The emission spectrum change of the WT reporter before (black) and after (red) PDGFRβ incubation. (**d-f**) The ratio time courses of WT reporter and its mutants as indicated. (**f**) inset shows the time course of zoom-in ratios of Y580F reporter upon PDGFRβ incubation. (**g**) The tyrosine phosphorylation of Y580 and Y542 of the WT reporter, its Y542F or Y580F mutant *in vitro* before and after PDGFRβ incubation. (**h**) The

models depict the *cis*-interactions and FRET changes of the WT and Y542F reporters upon phosphorylation *in vitro*.

Author Manuscript Author Manuscript Author Manuscript Author Manuscript

Author Manuscript Author Manuscript Author Manuscript Author Manuscript

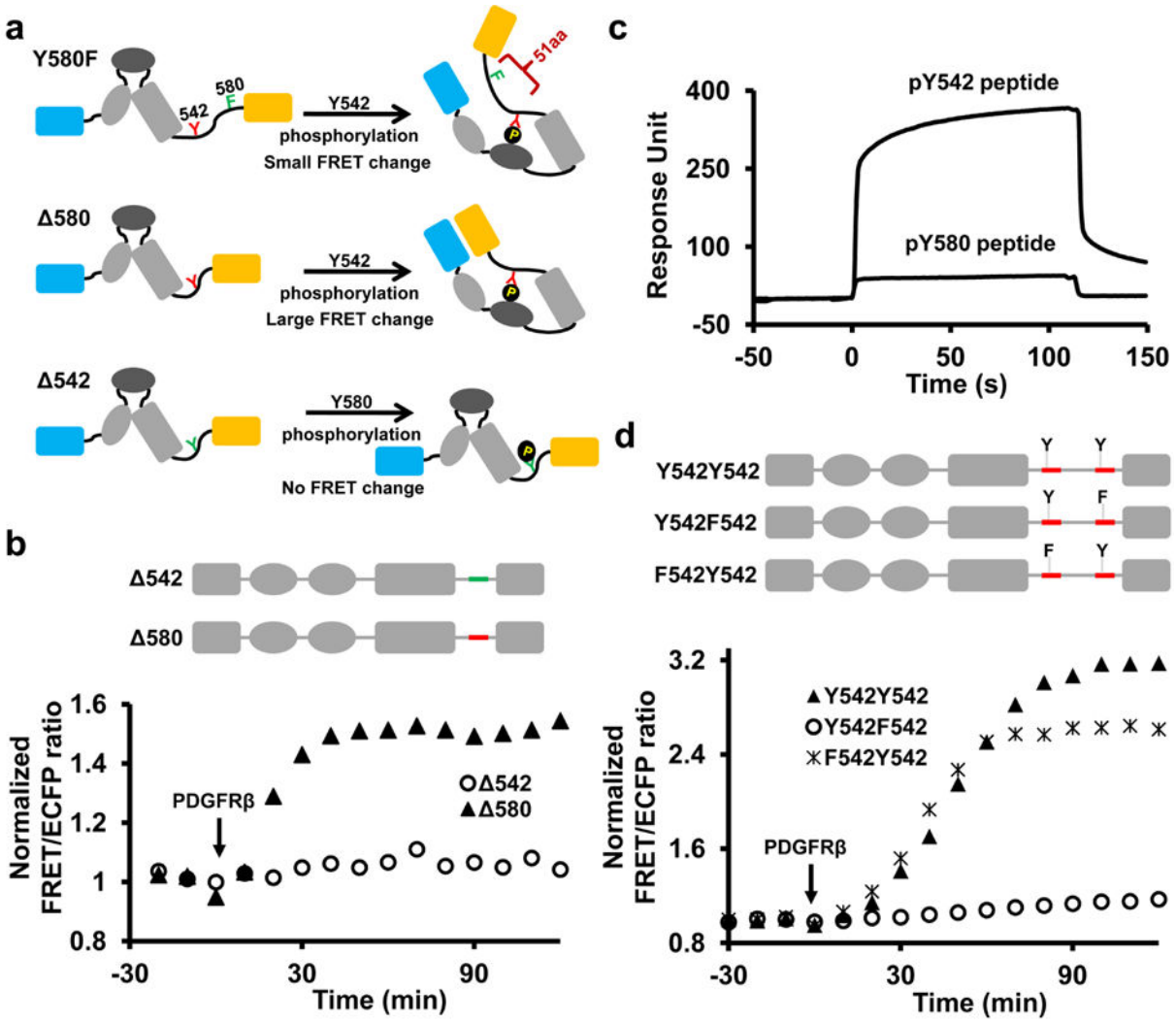

Figure 2. The combination of contextual sequence and position determines the preference of phosphotyrosines for *cis*-interaction

(**a**) The models depict the *cis*-interactions of the Y580F, Δ580 and Δ542 reporters upon phosphorylation *in vitro*. (**b**) The ratio time courses of Δ542 and Δ580 reporters. Y542 and Y580 sequences are colored in red and green, respectively. (**c**) The binding curves of the C-SH2 domain (4.5 μM) towards immobilized pY542 or pY580 peptides measured by SPR (refer to Supplementary Figure S8 for the binding kinetics and original sensorgrams). (**d**) The ratio time courses of engineered Y542Y542 and its mutant reporters as indicated.

Author Manuscript Author Manuscript Author Manuscript Author Manuscript

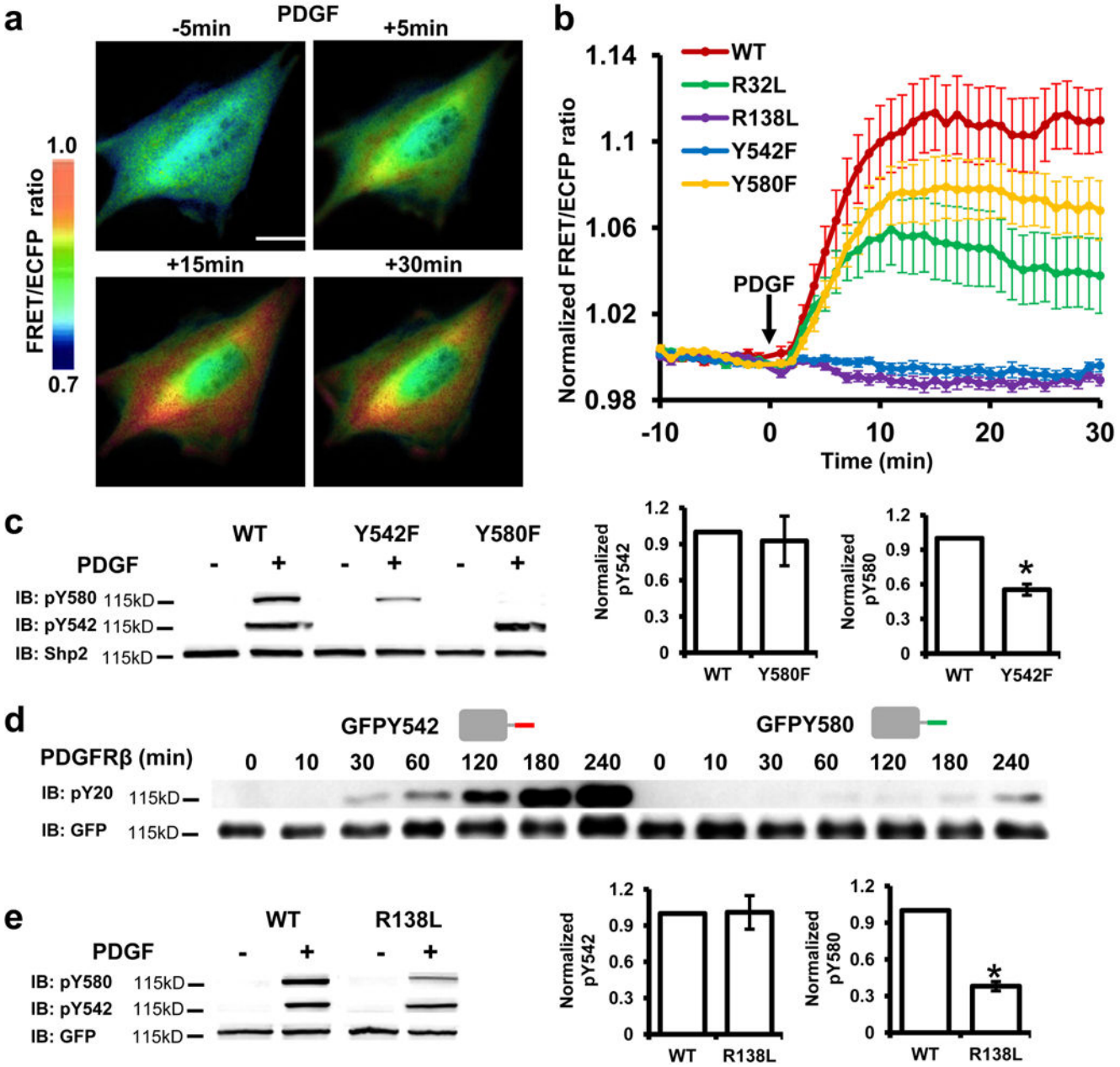

Figure 3. *cis*-Interactions and their regulation within the Shp2 reporters in MEFs

(**a**) The ratiometric images of a MEF cell transfected with the WT reporter before and after PDGF stimulation for various periods of time. Scare bar = 10 μm. (**b**) The ratio time courses (mean ± S.E.M, n=18, 17, 15, 15 and 11) of MEFs expressing the WT reporter or its mutants. (**c**) The phosphorylation of WT and tyrosine mutant reporters in MEFs before and after 5 min PDGF stimulation. Bar graphs represent the mean ± S.E.M. *, $P < 0.05$. (Student's t-test, n=3, refer to Supplementary Figure S6b for the whole blots). (**d**) The tyrosine phosphorylation levels of the purified GFPY542 (1 μM) or GFPY580 (1 μM) reporter before and after 10 nM PDGFRβ incubation for indicated time periods. (**e**) The phosphorylation of WT and C-SH2 mutant reporters in MEFs before and after 5 min PDGF

stimulation. Bar graphs represent the mean ± S.E.M. *, $P < 0.05$ (Student's t-test, n=3). Whole-cell lysate was used for panels (**c**) and (**e**).

Author Manuscript Author Manuscript Author Manuscript Author Manuscript

Author Manuscript Author Manuscript Author Manuscript Author Manuscript

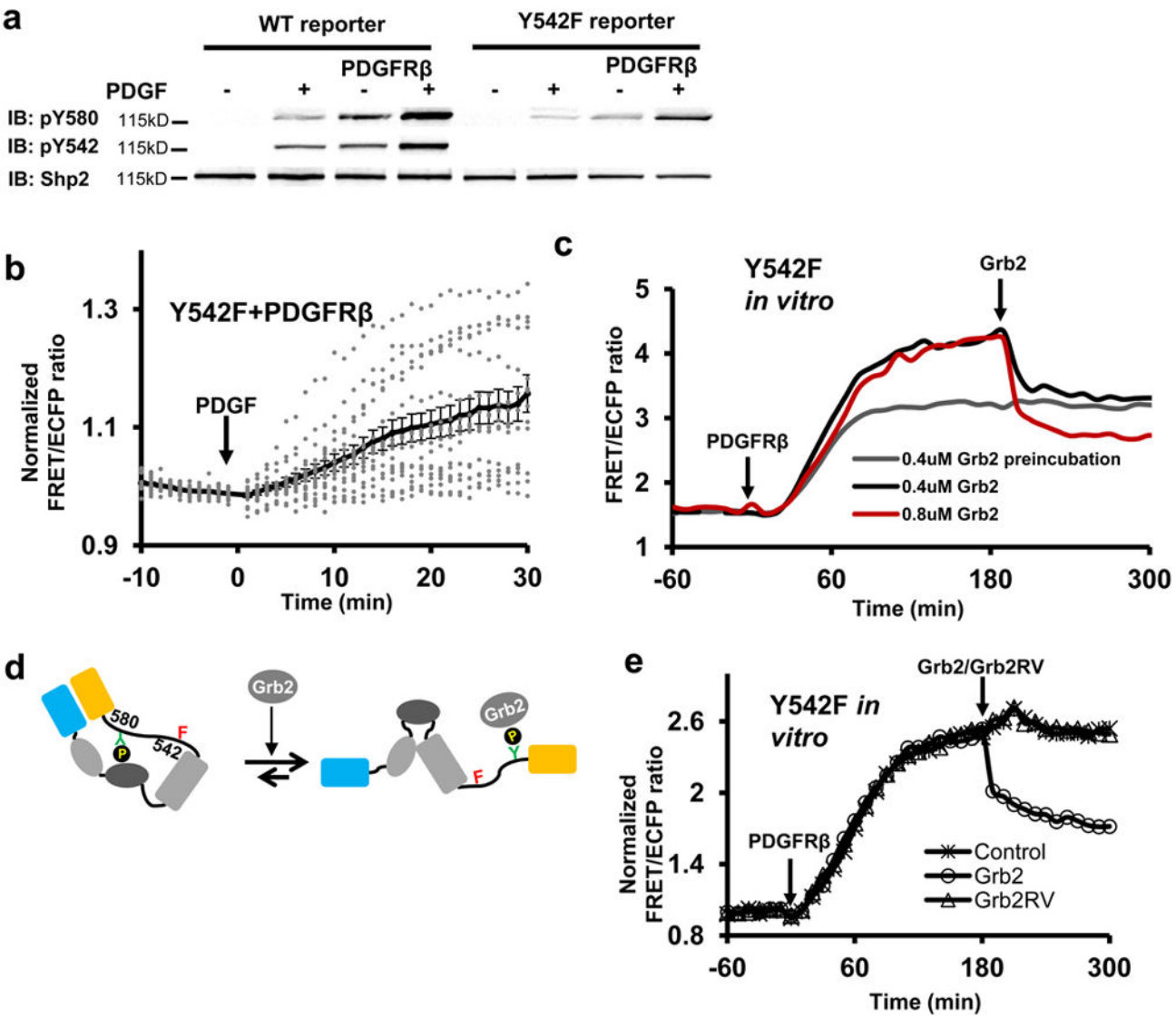

Figure 4. Grb2 can *trans*-interact with Shp2

(**a**) The phosphorylation of WT and Y542F reporters before and after 5 min PDGF stimulation in MEFs with or without the overexpression of PDGFRβ. (**b**) The ratio time courses of Y542F reporter before and after PDGF stimulation in MEFs overexpressing PDGFRβ. The dotted lines from each cell are overlaid with the solid curve (mean ± S.E.M.). (**c**) The PDGFRβ-induced ratio changes of Y542F reporter pre- or post-incubated with Grb2 *in vitro*. (**d**) The model depicts the effect of Grb2 in altering the Y542F reporter conformations. (**e**) The ratio time courses of the Y542F reporter *in vitro* upon PDGFRβ incubation, followed by the addition of Grb2 or Grb2RV.

Author Manuscript Author Manuscript Author Manuscript Author Manuscript

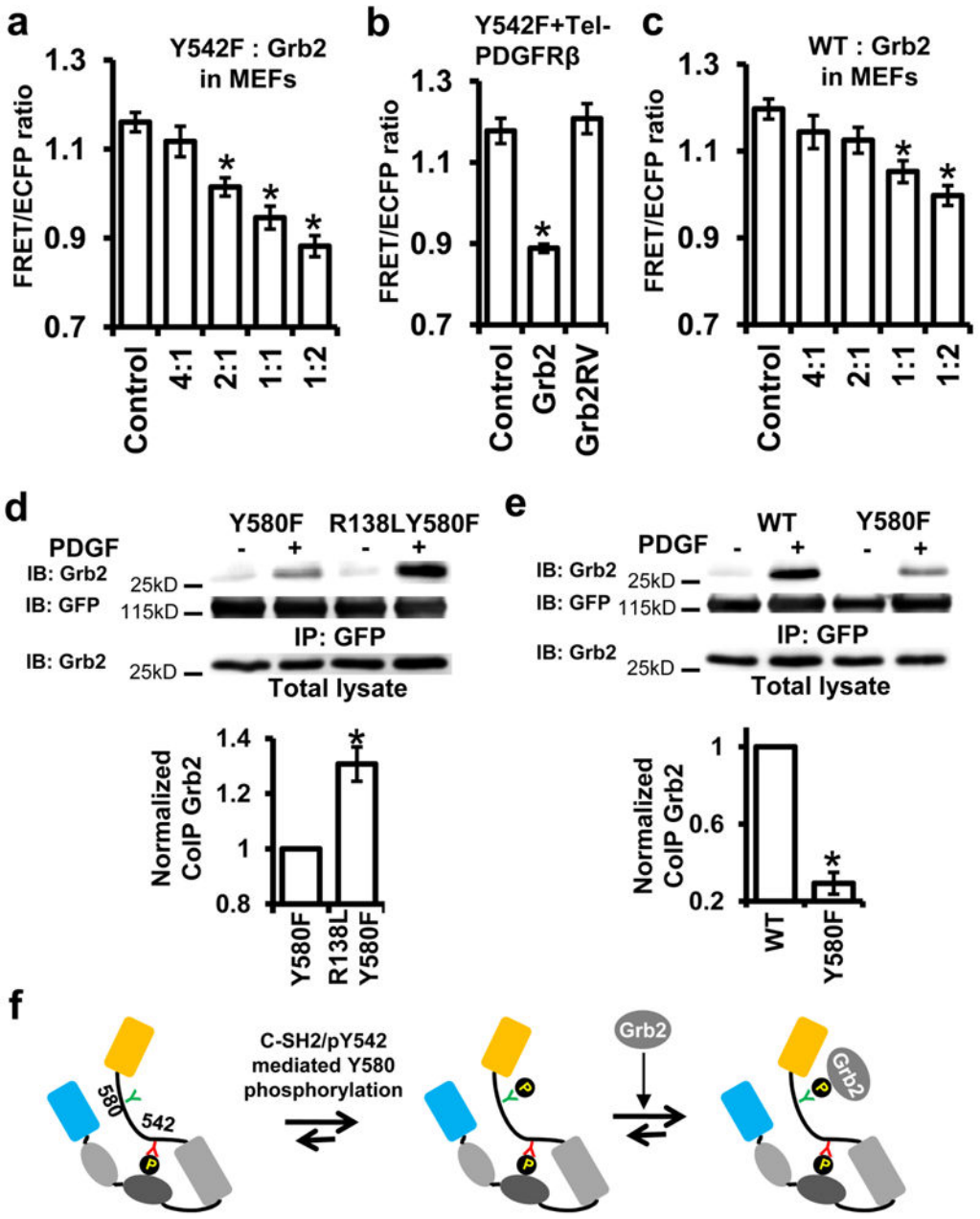

Figure 5. Grb2 tunes the *cis*-interaction of Shp2 in MEFs

(**a-c**) The averaged ratios of the Y542F (**a, b**) or WT (**c**) reporter in MEFs co-expressing Tel-PDGFRβ with control vector, different amounts of Grb2 (**a, c**), or Grb2RV (**b**). (**a**) n=16, 17, 14, 18, 11, *, P <4.55e-5; (**b**) n=38, 25, 26, *, P <1.0e-8; (**c**) n = 10, 20, 18, 15, 35, * P <3.1e-4 (Student's t-test with Bonferroni correction). (**d-e**) The amount of Grb2 co-immunoprecipitated with WT or its mutant reporters in MEFs before and after 15 min PDGF stimulation. *, P < 0.05 (Student's t-test, n=3). Bar graphs represent the mean ± S.E.M. of normalized intensity against its corresponding control group (refer to Supplementary Figure S7a for the whole blots). (**f**) The model depicts the early interaction of C-SH2/pY542, the

subsequent pY580 phosphorylation which recruits Grb2 and is sequestered by Grb2 to stabilize this C-SH2/pY542 pair.

Author Manuscript Author Manuscript Author Manuscript Author Manuscript

Author Manuscript Author Manuscript Author Manuscript Author Manuscript

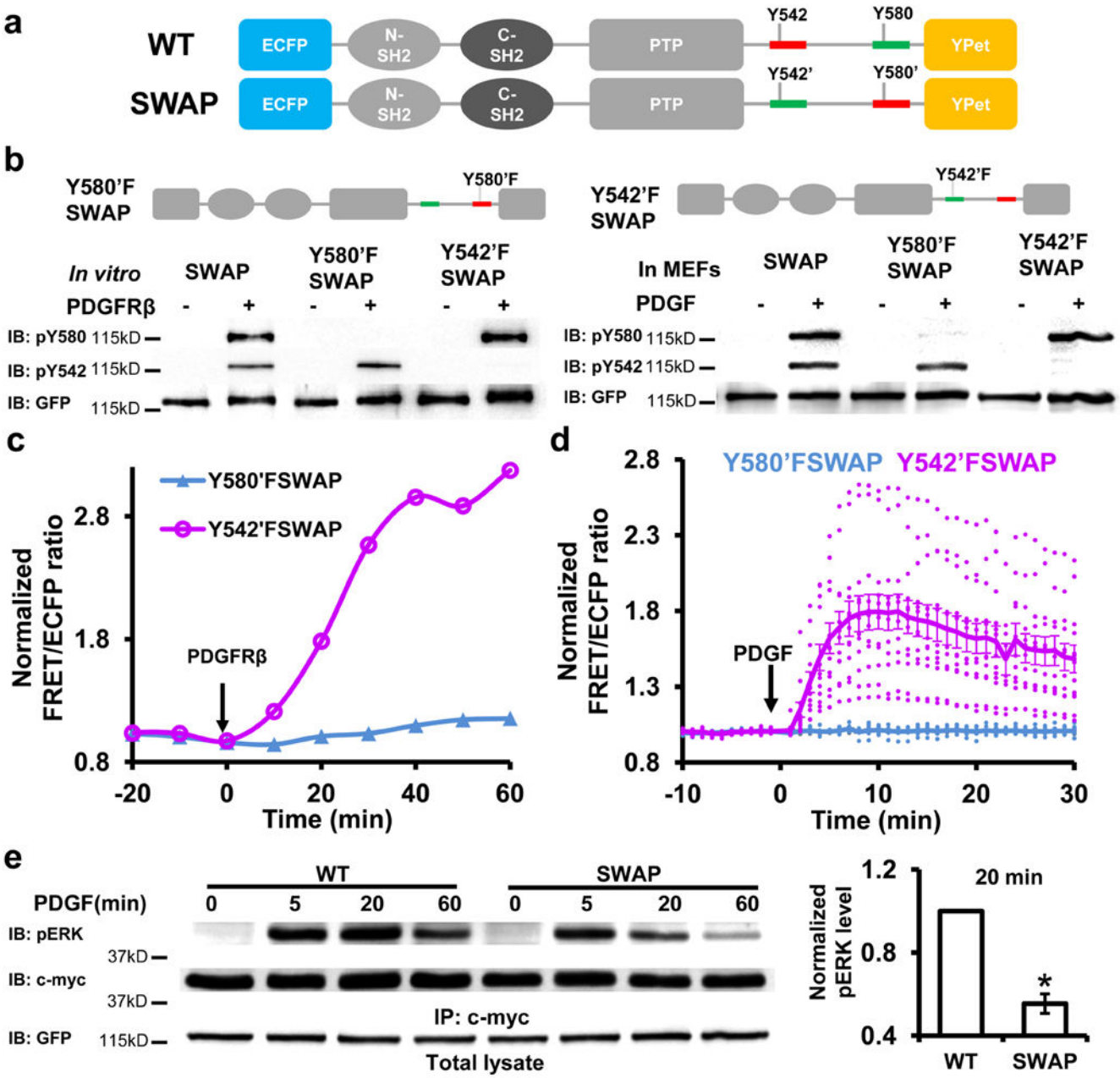

Figure 6. The loss of tunable *cis*-interaction within the SWAP reporter and its effect on ERK phosphorylation

(**a**) Schematic drawings and comparison of the WT and SWAP Shp2 reporters. Y542 and Y580 sequences are colored in red and green, respectively. (**b**) The phosphorylation of SWAP and its mutant reporters *in vitro*(Left) or in MEFs (Right, whole cell lysate). (**c-d**) The ratio changes of Y542'FSWAP and Y580'FSWAP reporters (**c**) *in vitro* or (**d**) in MEFs. (**e**) The ERK phosphorylation at different time points (left) and its quantification (mean ± S.E.M.) at 20 min (right) upon PDGF stimulation in MEFs expressing either WT or SWAP reporter as indicated. *, $P < 0.05$ (Student's t-test, n=3, refer to Supplementary Figure S7b for the whole blots).

Author Manuscript

Author Manuscript

Author Manuscript

Author Manuscript

Table 1

The dissociation constant (K_d) of different peptides toward the binding of Grb2 or C-SH2 domain of Shp2

Peptide name	Peptide sequence[a]	C-SH2 K_d (μM)	Grb2 K_d (nM)
pY542	KGHEpYTNIKYS	15.1 ± 0.47	118 ± 10.3
pY580	SARVpYENVGLM	294 ± 23.6	68.5 ± 8.7

[a] All peptides contain a biotin-ASASA at their N termini